Molecular Mobility and Physical Ageing of Plasticized Poly(lactide)

Larisa Dobircau,[1] Nicolas Delpouve,[1] Romuald Herbinet,[2] Sandra Domenek,[3] Loïc Le Pluart,[2] Laurent Delbreilh,[1] Violette Ducruet,[4] Eric Dargent[1]

[1] *AMME-LECAP EA4528 International Laboratory, Institut des Matériaux de Rouen, Université et INSA de Rouen, BP12, 76801 Saint Etienne du Rouvray Cedex, France*

[2] *Laboratoire de Chimie Moléculaire Thio-organique (LCMT), UMR 6507, INC3M, FR3038, Ensicaen & Université de Caen, 6 boulevard du Maréchal Juin, 14050 Caen, France*

[3] *AgroParisTech, UMR1145 Ingénierie Procédés Aliments, 1 Avenue des Olympiades, 91300 Massy, France*

[4] *INRA, UMR1145 Ingénierie Procédés Aliments, 1 Avenue des Olympiades, 91300 Massy, France*

Molecular mobility and physical ageing of amorphous plasticized polylactide (PLA) with two different contents of mesolactide are studied with the help of thermal analysis. Used plasticizers are acetyl tributyl citrate (ATBC) and triacetin (TA), two molecules with established miscibility and plasticizing efficiency. Lower plasticizer permanence of TA compared with ATBC is found. The plasticizer molecules decreased the size of the cooperativity domains at the glass transition temperature T_g and likely in the glassy state by decreasing intermacromolecular interactions and notwithstanding the mesolactide content of PLA and the chemical identity of the plasticizer. The recovery function is given and shows a significant effect of the plasticizer on the physical ageing. The supplementary free volume brought by the plasticizer enhances molecular mobility in the glassy state and increases structural relaxation at one order of magnitude. The comparison between different plasticizers reveals that the structural relaxation is however independent from the type of plasticizer and the percentage of mesolactide in PLA. POLYM. ENG. SCI., 55:858–865, 2015. © 2014 Society of Plastics Engineers

INTRODUCTION

There is considerable interest for the elaboration of biodegradable and/or biosourced packaging materials to replace plastics engineered by petrochemistry, because packaging represents a high volume market [1]. Poly(lactide) (PLA) is one of the most studied polymers in this respect, because it is a biobased and biodegradable polyester with a glass transition temperature higher than room temperature (~60°C). PLA is easily processable, and has interesting use properties such as high transparency and gloss, sealing and printing ability, high tensile modulus. It is however a brittle polymer with a moderate yield strength and small elongation at break [2]. To overcome its brittleness, external, and internal plasticizing are extensively investigated [3, 4]. External plasticizing consists in the melt mixing of the polymer with a plasticizer, typically a high-boiling point, viscous, and miscible liquid. Numerous molecules used for external plasticizing of PLA have shown to be efficient in terms of increase of elongation at break and decrease of glass transition temperature (T_g) [3–6]. Although plasticizer permanence in the material is one big challenge for external plasticizing, ageing studies of plasticized PLA under controlled environmental conditions are very scarce. It has been observed that the storage of PLA/TA at room temperature, thus almost at T_g, showed cold crystallization of the polymer after 123 days [7]. Courgneau et al. [8] showed by electron spin resonance for PLA/ATBC that a local demixing phenomenon and plasticizer migration to the surface happens during sample ageing beyond glass temperature at concentrations higher than 10 wt%. Hassouna et al. [9] investigated the ageing of PLA/ATBC systems at 20°C (almost at T_g) for 6 months. They found that T_g decreases during ageing. The explanation is that crystallization of PLA during the ageing period might lead to the expulsion of the plasticizer from the crystalline lamellae and thereby to its enrichment in the amorphous phase. As the distance between T_g and ageing temperature in these studies is not controlled, comparison of ageing behavior between plasticizers is impossible.

Furthermore, ageing of plasticized PLA at controlled distance to T_g in the glassy state has not been studied yet. In glasses, the excess of enthalpy, entropy and free volume present is removed via structural relaxation to reach the thermodynamic equilibrium state [10, 11]. This slow and gradual approach called physical ageing leads among others to increase in yield stress and gas barrier properties and embrittlement of the polymer [12]. The structural relaxation is nonlinear and nonexponential as generally captured within the frameworks of TNM [13–15] and KAHR [16]. The time scales required to reach equilibrium for volume recovery and stress relaxation have been extensively studied by McKenna et al. [17–20]. However, the nature itself of physical ageing in polymers is still an open question and many works aiming to understand the molecular dynamics in the glassy state are mentioned in the literature [21–25]. For instance, Drozdov [26] proposed that the structural relaxation in a disordered medium is governed by two processes at the macromolecular scale: fragmentation and aggregation of the Cooperative Rearranging Regions (CRR). The CRR represents the smallest amorphous domain allowing for conformational rearrangement without causing structural change at its boundary [27]. Physical ageing has been extensively studied for neat PLA [28–32], showing effects such as increasing embrittlement [32] and decelerating enzymatic degradation [28], both explained by the appearance of locally ordered domains [29, 30].

The aim of this work is to study for the first time the influence of plasticizers on physical ageing and molecular dynamics at the glass transition under thoroughly controlled conditions in

Correspondence to: Eric Dargent; e-mail: eric.dargent@univ-rouen.fr
DOI 10.1002/pen.23952
Published online in Wiley Online Library (wileyonlinelibrary.com).

TABLE 1. Characteristics of the plasticizers.

	M (g mol^{-1})	V_m (cm^3 mol^{-1})	T_g DSC (°C)	δ [(MJ m^{-3})$^{0.5}$]	x (%)
TA	218	188	−70	19.4	61
ATBC	402	384	−82.5	18.4	44

M: molecular weight; V_m: molar volume; T_g: mid-point glass transition temperature; δ: Hildebrand solubility parameter; x%: weight proportion of ester groups.

a calorimeter and at a fixed distance to T_g. Two different plasticizers and two different grades of PLA are used for gathering information on the influence of chemical parameters on the structural relaxation. To avoid differences among samples due to variable degrees of crystallinity, all the materials of this work are strictly amorphous. The influence of plasticizing on the molecular mobility in formulated PLA is discussed by analyzing CRR size at the dynamic glass transition, in comparison to neat PLA using the approach taken in previous papers [33–35]. Quantitative results on the influence of the plasticizer on the size of the cooperative domains are given.

EXPERIMENTAL

Materials

PLAs with an average meso-lactide content of 5.2% are provided by NaturePlast (PLA-5, Caen, France) and of 8% by NatureWorks (PLA-8). Triacetin (TA, CAS Number 102-76-1) is obtained from Fluka (France) and Acetyl tributyl citrate (ATBC, CAS Number 77-90-7) from Sigma Aldrich (France). The characteristics of both plasticizers are given in Table 1.

PLA-5 and TA are dried at 50°C under vacuum during 24 h before processing. Processing experiments are performed with a 15 cm^3 DSM Xplore (Geleen, Netherlands) corotating twin screw μ-extruder. The barrel temperature is set at 200°C and the screw speed at 100 rpm. PLA-5 is melt blended with 5 and 10 %wt of TA during 2 min. Then, the blend is injected and molded with an Xplore 10 cm^3 injection unit in a mold whose temperature is set at 30°C to obtain normalized tensile testing dog bone samples (ISO-527-2-5A).

PLA-8 and ATBC are dried at 80°C under vacuum for 12 h. Blending is performed with an internal mixer (Haake Rheocord 9000) at 160°C and 60 rpm for 15 min. After a subsequent drying step (4 h at 80°C under vacuum) samples are thermomolded between two hot plates under 10 bars for 2 min and quenched to room temperature. Both processing procedures yielded amorphous samples.

The average number (M_n) and weight (M_w) molecular weights have been measured by size exclusion chromatography calibrated with polystyrene standards. Experiments were carried out at 37°C in THF with Waters Styragel columns. The detector was a differential refractive index (Waters 410). The average molecular weights (M_n) are 95000 g mol^{-1} (dispersity 1.8) for PLA-5 and 90500 g mol^{-1} (dispersity 2.75) for PLA-8.

Differential Scanning Calorimetry (DSC)

DSC analyses are performed on all the samples at 10°C min^{-1} from 0 to 200°C with DSC 2920 (TA® instruments) equipped with a Refrigerating Cooling System. The calibration in temperature and energy are done using standards of indium (T_{fusion} = 156.6°C) and benzophenone (T_{fusion} = 48.0°C). Samples are disposed in aluminum pans to allow the best thermal contact possible. Nitrogen is used as sweep gas with a flow of 70 mL min^{-1}. The sample masses are around 10 mg. The given glass transition temperatures are calculated at mid-height of the heat flow step.

Temperature Modulated Differential Scanning Calorimetry (TMDSC)

TMDSC analyses are carried out on zero-aged samples in DSC Q100 (TA® instruments) in the same temperature range than classical DSC. The specific heat capacity calibration is made using sapphire as reference. Experiments are performed under nitrogen atmosphere (70 mL min^{-1}) with oscillation amplitude of 1.5°C, a period of 80 s and a heating rate of 1°C min^{-1}. These conditions correspond to the heat cool mode and are required for a clear analysis of the glass transition. The modulation step number is estimated higher than five during the glass transition. The complete deconvolution procedure is done as proposed by Reading [36] and the phase angle correction as proposed by Weyer et al. [37]. Before performing the TMDSC, the thermal history of the samples is erased by heating them at 10°C min^{-1} up to a temperature just above the glass transition range to prevent crystallization and immediately cooling down to 0 at 10°C min^{-1} to limit at maximum any risk of plasticizer migration. From TMDSC, different signals can be obtained: the heat flow and the apparent complex heat capacity C^*. From the ratio between the amplitude of the modulated heat flow A_q and the amplitude of the heating rate A_β, C^* can be calculated according to *Eq. 1*:

$$|C^*| = \frac{A_q}{A_\beta} \times \frac{1}{m} \tag{1}$$

where m is the sample mass. Due to the phase lag φ between the calorimeter response function (i.e., the heat flow) and the time derivative of the modulated temperature program, two components (the in-phase and out-of-phase components of the apparent complex heat capacity) noted, respectively, C' and C'' can be calculated according to *Eqs. 2* and *3*:

$$C' = C^* \cos\varphi \tag{2}$$

$$C'' = C^* \sin\varphi. \tag{3}$$

In this study, the in-phase component C' and the out-of-phase component C'' are analyzed. The C' versus temperature variation in the glass transition temperature region appears usually as an endothermic step whereas C'' variation displays a peak. Since the ageing history has a strong influence on the form of the C'' signal [38], only non-aged samples are characterized with TMDSC. For both DSC and TMDSC, the uncertainties on temperature are ± 0.5°C and on the heat capacity step ± 0.04 J g^{-1} K^{-1}.

Physical Ageing

Physical ageing is carried in situ under nitrogen atmosphere at ageing temperature T_a equal to T_g – 15 °C for each composition. This is a classical procedure for observing the enthalpy

TABLE 2. Glass transition characteristics of plasticized PLA measured by DSC and TMDSC.

	T_g DSC (°C)	T_g Fox (°C)	ΔCp (J g^{-1} K^{-1})	$\Delta H\infty$ (J g^{-1})	T_α TMDSC (°C)	δT (°C)	$\xi_{T\alpha}$ (nm)
PLA-5	60	60	0.46	6.9	59	3.0	2.8
PLA-5+5% TA	51	50	0.50	7.5	48	3.6	2.5
PLA-5+10% TA	38	40	0.42	6.3	38	4.6	2.1
PLA-8	60	60	0.55	8.3	55	2.8	3.0
PLA-8+5% ATBC	50	48	0.46	6.9	48	3.5	2.6
PLA-8+10% ATBC	41	37	0.45	6.8	40	4.3	2.2

T_g: mid-point glass transition temperature; T_g: FOX theoretical mid-point glass transition temperature with respect to the Fox law, ΔCp: heat capacity step at T_g; $\Delta H\infty$: enthalpy of recovery for an infinite duration of ageing; T_α: maximum of the out-of-phase C″ peak, δT: the mean temperature fluctuation related to the dynamic glass transition of one CRR, $\xi T\alpha$: CRR size at the dynamic glass transition temperature.

relaxation process of polyesters in the glassy state [35, 39, 40]. The atmosphere is kept under nitrogen to prevent any chemical ageing induced by oxygen or humidity [41]. The T_g of non-aged amorphous PLA are reported in Table 2. To prevent recrystallization, the DSC heating scan is stopped immediately after PLA had passed its glass transition. The lowest T_g values (for PLA + 10%wt plasticizer) lead to ageing temperature close to room temperature (T_a are 23 and 26°C for PLA-5 + 10%wt TA and PLA-8 + 10%wt ATBC, respectively). At the end of the ageing cycle, the amorphous nature of the materials is checked by heating over PLA melting temperature. Physical ageing times t_a varied from 0 to 150 h (0, 0.17, 1, 3, 5, 10, 20, 50, 100, and 150 h). Consequently, two ageing procedures are experimented during this work: the first procedure consists in analyzing the same sample for all the ageing times of a given material (Fig. 1a). The sample is heated over temperature of fusion and quenched between each ageing period to avoid crystallization, which could occur at $T > T_g$. As a consequence, the DSC oven is not opened, no changes of the sample mass and of the thermal contact (position of sample) can occur. This procedure minimizes uncertainty linked to DSC apparatus and the wholly amorphous state of samples is maintained. The drawback of this method is the repeated heating of the same sample which might induce thermal degradation of PLA and plasticizer. The second procedure (Fig. 1b) consists in using a different sample for each ageing time. As a consequence, the sample mass can vary (± 2 mg) and thermal contact could change due to change of sample (position and mass). The interest of this second procedure is that a new wholly amorphous sample is used for each ageing period. In case of both procedures, the sample is cooled down to room temperature at 50°C min^{-1} after the DSC scan of the glass transition of the aged sample in the aim to perform a second heating scan on the rejuvenated material. This second heating scan is compared to the very first heating scan of the non-aged sample to check for changes in glass transition due to thermal degradation.

RESULTS AND DISCUSSION

CRR Size of Plasticized PLA

To investigate the influence of the plasticizing molecules on the molecular mobility of PLA, standard DSC and TMDSC analysis are performed on each material. The T_g and the heat capacity step at T_g (ΔC_p), both measured by standard DSC (heating at 10°C min^{-1}), are reported in Table 2. In accordance with the literature [42] the two neat PLA exhibit a T_g at 60°C. A shift of T_g towards lower values occurs for the plasticized PLA. As expected, the action of the plasticizer is to induce higher chain mobility at lower temperature. The T_g values of PLA-8/ATBC and PLA-5/TA systems are consistent with the theoretical T_g calculated from the well-known Fox equation and presented in Table 2. Comparison of T_g values shows moreover that the plasticizing efficiency of TA is better than the one of ATBC. When adding 10%wt plasticizer, T_g decreases from 60 to 38°C for the PLA-5/TA while it decreases from 60 to 41°C for the PLA-8/ATBC. Similar observations have been reported

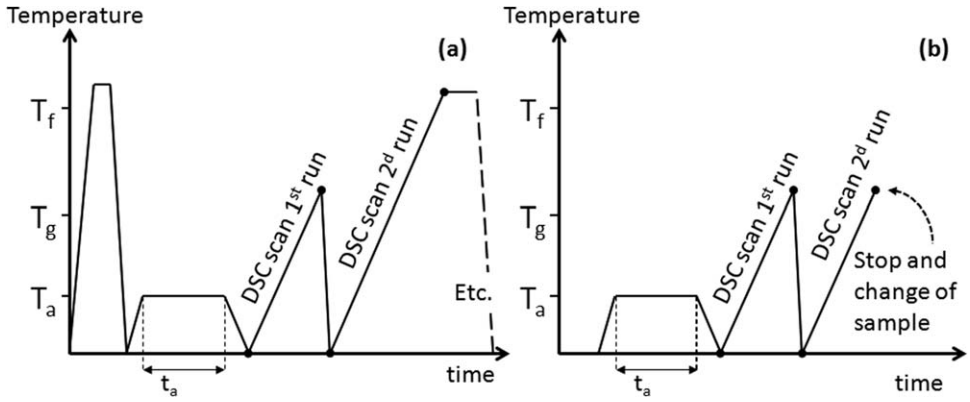

FIG. 1. Temperature versus time schemes for the physical ageing procedure. T_a, T_g, and T_m are, respectively, the annealing temperature, the glass transition temperature measured on a nonaged sample, and the fusion temperature. (a) Procedure 1, one same sample for the different ageing times and (b) procedure 2, a different sample for each ageing time.

 DOI 10.1002/pen

in the literature with ATBC yielding T_g values between 45 and 47°C at a content of 10 wt% [9, 43–46] and between 17 and 38°C at a content of 20 wt% [9, 43–45, 47, 48] while TA decreases T_g from 60°C (neat PLA) to values between 29 to 48°C at a content of 10 wt% and between 21 to 29°C at 20 wt% [7, 44, 46, 49]. Plasticization is typically dependent on the chemical nature of the molecule [50]. As reported by Ljungberg et al. [51], the reason of the good solubility of citrate derivatives and TA in PLA is probably caused by polar interactions between the esters groups of the plasticizer and PLA. The proportion of ester groups in TA and ATBC are 61 and 44% w/w, respectively. Solubility parameters are useful for the prediction of the miscibility of a given molecule with PLA [3]. As shown in Table 1, the Hildebrand solubility parameter of PLA is [21.9 (MJ m^{-3})$^{0.5}$]. Most probably because of its higher polarity compared to ATBC, TA has a closer Hildebrand solubility parameter to PLA: [19.4 (MJ m^{-3})$^{0.5}$] for TA versus [18.4 (MJ m^{-3})$^{0.5}$] for ATBC. The influence of the plasticizer addition on the change of heat capacity at the glass transition is less visible. For the PLA-8/ATBC blend, ΔC_p decreases from 0.55 to 0.45 J g^{-1} K^{-1} when the content of plasticizer reaches 10%. In the case of PLA-5/TA blend, the discrepancy of the data does not allow speculating about the magnitude of the heat capacity step. This suggests that the PLA-5/TA is a weak stability system reducing the reproducibility of the calorimetric measurement. Furthermore, for all systems, the differences of ΔC_p between the six samples are close to uncertainty (± 0.04 J g^{-1} K^{-1}). As already mentioned all the studied systems are amorphous so the variations of ΔC_p are purely related to the amorphous phase organization. It is assumed that in this study, the content of plasticizer is too low to afford significant variations of ΔC_p.

The molecular mobility of plasticized non-aged samples is investigated with TMDSC using the CRR concept. According to Donth's approach [52], the characteristic volume of cooperativity at the dynamic glass transition temperature T_α noted $\xi^3_{T\alpha}$, can be estimated from the following equation:

$$\xi^3_{T\alpha} = \frac{\Delta(1/C_p)}{\rho(\delta T)^2} k_B T_\alpha^2 \quad (4)$$

with δT the mean temperature fluctuation related to the dynamic glass transition of one CRR [53], k_B the Boltzmann constant, ρ the polymer density, and C_p the heat capacity at constant pressure (determined from C' signal). C' curves of first and second heating scans are similar and bring no further information compared with standard DSC. That is why they are not shown here. Figure 2 shows the temperature shift of the C'' peak to lower temperatures when the plasticizer content increased. T_α values are reported in Table 2. As already discussed in literature T_g is slightly lower than T_α [54, 55]. The C'' peak broadens with plasticizer content (Fig. 2), resulting in the increase of the mean temperature fluctuation δT (Table 2) which corresponds to the standard deviation of the C'' Gaussian fit. In PLA-5, it increases from 3.0 to 4.6°C when adding 10% TA and it increases from 2.8 to 4.3°C in PLA-8 when adding 10% ATBC. This causes the decrease of the CRR average size, as calculated by *Eq. 4* and given in Table 2. The volume of a CRR (ξ^3) varies in the same range than those calculated for other glass-formers [56–61]. It decreases of about 60% as the percentage of TA or ATBC reached 10 %wt. Obviously one could expect that different matrix exhibit different final relaxation properties. However the values of T_α, δT, and $\xi^3_{T\alpha}$ in PLA-5 and PLA-8 are too close to consider significant variations. This will help to distinguish which variations observed for plasticized materials are relevant. Since both molecular weight and stereoregularity differences do not cause any change in relaxation parameters, one can consider that the changes associated to the plasticization reveal a strong modification of the amorphous phase organization. As supported by a study of Dlubek et al. [62] in particular by means of Positron annihilation lifetime spectroscopy the addition of plasticizer in a macromolecular matrix increases the free volume and thereby the chain mobility. However, no significant differences in ξ^3 are noticed between TA and ATBC blends, although the molar volume of both plasticizers (188 cm^3 mol^{-1} for TA and 384 cm^3 mol^{-1} for ATBC) and the polar interaction of the molecules with the PLA chain is supposedly be different. Apparently, the interplay of both parameters brings about the same change in molecular mobility.

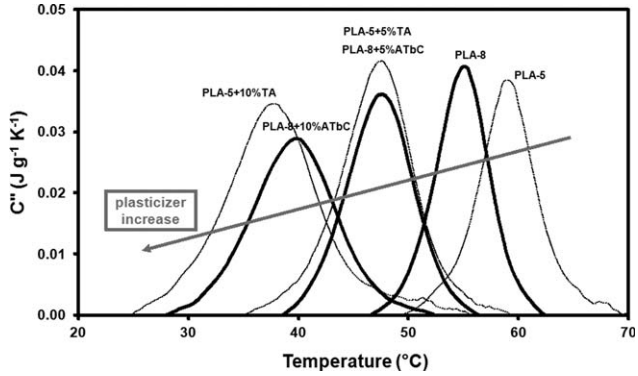

FIG. 2. Out-of-phase C″ curves from TMDSC analysis for six samples. Bold curves: PLA-8/ATBC; dotted curves: PLA-5/TA

Physical Ageing of Plasticized PLA

Long term stability and plasticizer permanence in the material are important features for successful compounding. As mentioned in the introduction, some studies have been performed on the ageing of PLA/ATBC and PLA/TA blends at room temperature. Concluding about those studies is however not straightforward, as the distance of the storage temperature with respect to the T_g of the plasticized material changed with the plasticizer content. Long term stability analysis is therefore carried out at temperatures slightly below, beyond or at glass transition. In the aim to avoid this issue, ageing of the samples is carried out in this study in a DSC oven at a fixed distance from T_g, exactly at $T_g - T_a = 15$°C using the procedures displayed in Fig. 1.

Figure 3 shows the second heating scans obtain by the procedure 1 (Fig. 1a) for PLA-8/ATBC for ageing times up to 150 h. No variation of the glass transition temperature range, glass transition temperature, or heat capacity step is detected after ageing. We deduce that ATBC is stable in the PLA-8 matrix even after several heating cycles to temperatures above PLA fusion temperature (T_f). The same procedure 1 is used to analyze PLA-5/TA. Figure 4 shows that the second heating scans are reproducible for the neat PLA but not for the plasticized polymer. After each ageing and heating cycle above T_f, the glass transition temperature increases without significant variation of

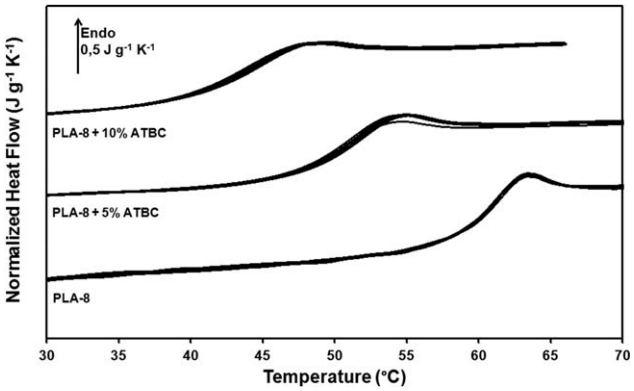

FIG. 3. Second DSC runs for PLA-8/ATBC [procedure 1, $T_a = 26°C$, Ageing times varied from 0 to 150 h (0, 0.17, 1, 3, 5, 10, 20, 50, 100, and 150 h)].

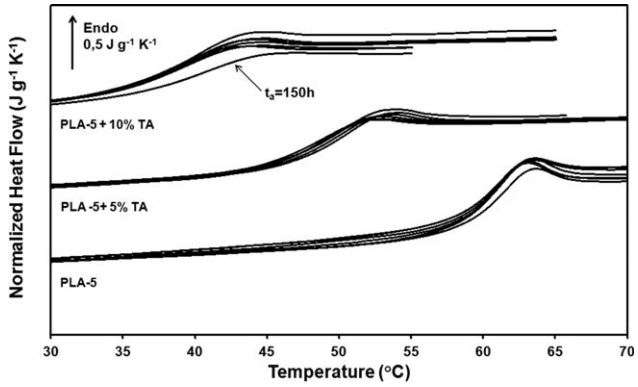

FIG. 5. Second DSC runs for PLA-5/TA [procedure 2 $T_a = 26°C$, Ageing times varied from 0 to 150 h (0, 0.17, 1, 3, 5, 10, 20, 50, 100, and 150 h)].

the heat capacity step. After five cycles, the glass transition is close to the one of neat PLA-5 (~60°C). A change of crystallinity degree would have induced an increase of T_g and a decrease of the heat capacity step [33, 34]. ΔC_p is however constant. Therefore the increase of the glass transition temperature cannot be attributed to a modification of the crystallinity degree. Obviously, using procedure 1, the PLA-5/TA blends are not thermally stable and a loss of plasticizer is observed. TA has a lower molecular weight (218 versus 402 g mol^{-1} for ATBC) and a lower boiling point that ATBC (258 vs. 441°C), which can explain the lower permanence. As a consequence, the procedure 2 is tested for PLA-5/TA (procedure 1 is kept for PLA-8/ATBC due to the better reproducibility of the DSC signals). The second heating runs (Fig. 5) validated good signal reproducibility of procedure 2 for neat PLA and PLA-5 +5 %wt TA. For the PLA-5 +10 %wt TA, no variation in glass transition is observed until $t_a = 100$ h. For the longest ageing time ($t_a = 150$ h) a small but significant increase of the glass transition temperature occurs, probably due to the loss of TA during ageing in the oven.

Typical first heating scans of the aged samples are reported on Fig. 6 using the example PLA-8 +10 %wt ATBC. One observes the growth of the endothermic relaxation peak with ageing time and the shift of the peak maximum T_p to higher temperatures typical for short ageing times, as already observed for other systems [12, 22]. As reminded by Lixon Buquet et al. [63] the usual procedure allowing the calculation of the recovery enthalpy (ΔH) consists in subtracting the curve of the second heating run from the one of the first heating run then in integrating the difference. This value corresponds to the energy needed by the glass to reach the thermodynamic equilibrium. ΔH is reported in Fig. 7 as a function of the ageing time. It can be seen that the variations of ΔH are similar for the different plasticized PLAs probed. In literature, the nonexponential and nonlinear behavior of physical ageing is established [13–17, 22, 24, 64, 65] and the enthalpy recovery phenomena can be described following the *Eqs. 5* and *6*:

$$\frac{\Delta H_\infty - \Delta H(t_a)}{\Delta H_\infty} = \exp\left[-\left(\frac{t}{\tau}\right)^\beta\right] \quad (5)$$

$$\tau = A\exp\left[\frac{x\Delta h^*}{kT_a} + \frac{(1-x)\Delta h^*}{kT_f}\right] \quad (6)$$

where $\beta < 1$ is the stretching exponent, τ is a characteristic relaxation time, A is a pre-exponential factor, x is the nonlinearity parameter, Δh^* is the Tool-Narayanaswamy-Moynihan activation energy, and T_f is the fictive temperature. In theory, after an infinite ageing time performed on a glass maintained at a temperature $T_a < T_g$, but close to T_g, the expected enthalpy loss ΔH_∞ can be estimated by means of the *Eq. 7*:

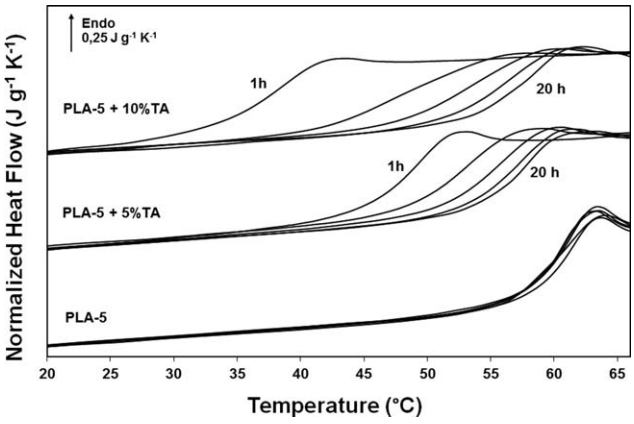

FIG. 4. Second DSC runs for PLA-5/TA [procedure 1, $T_a = 23°C$, Ageing times varied from 1 to 20 h (1, 3, 5, 10, and 20 h)].

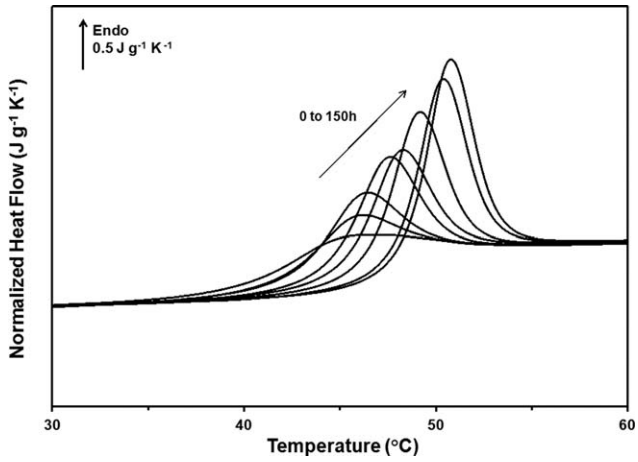

FIG. 6. Normalized heat flow for PLA-8 + 10 wt% ATBC. First DSC runs with procedure 1 ($T_a = 26°C$, Ageing times varied from 0 to 150 h (0, 3, 5, 10, 20, 50, 100, and 150 h).

DOI 10.1002/pen

$$\Delta H_\infty = \Delta C_p (T_g - T_a) \quad (7)$$

Here, as shown in Table 2, ΔH_∞ values average at about 7.1 ± 1.2 J g^{-1} without any visible tendency related to the plasticizer quantity. One can note that the variations of ΔH for a material should be considered in respect to the associated ΔH_∞ values. To compare the enthalpy recovery kinetics for the different samples, the recovery function $\phi(t_a)$ is calculated according to *Eq. 8* and plotted in the Fig. 8 as a function of ageing time:

$$\varphi(t_a) = \frac{\Delta H_\infty - \Delta H(t_a)}{\Delta H_\infty} \quad (8)$$

For non-aged samples (very short time) $\phi(t_a)$ is equal to 1, while for fully recovered enthalpy $\phi(t_a)$ is equal to 0 ($\Delta H = \Delta H_\infty$). The recovery functions have quite similar shapes for the neat and the plasticized PLA. It should be noted that the recovery function never reached the limit of 0.5 even for the longest ageing times. This value is far from the predicted final value [$\phi(t_a) = 0$] because the chosen ageing times are not sufficiently long to reach thermodynamic equilibrium. It can be assumed that PLA and plasticized PLA recovery processes are similar to other polymers. In literature, $\Delta H(t_a)$ values of some amorphous polymers are in the range 37–75% of the ΔH_∞ after 100 h for the same ageing conditions ($T_a = T_g - 15$°C) [63]. The recovery function for neat PLA and plasticized PLA are different. As shown in the insert on Fig. 8, the recovery process occurs at lower times for plasticized PLA. The decrease is small (one decade) but significant. As a consequence one can note that even in the glassy state, the plasticizer modifies the macromolecular motions and a reduction of the time needed for cooperative motions occurs due to the breaking of interactions between macromolecular chains. The accelerating effect of the plasticizers on the molecular mobility can thus be observed in the glassy state. The increase of molecular motions is also indicated for plasticized PVC by Gomez-Ribelles et al. [66] and matches with the behavior of stacked ultrathin films undergoing T_g depression [67]. As a clear relationship has been established between molecular mobility rate and cooperativity length scale [68–70], we assume that the CRR size decreases in the glassy state as the percentage of plasticizer increases. This decrease supports the decrease of CRR size of plasticized PLA observed at T_g and is concordant with the idea developed by several

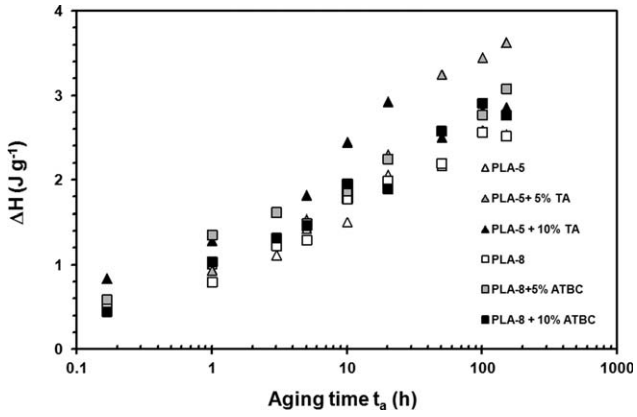

FIG. 7. Variations of the enthalpy of recovery as a function of the ageing time.

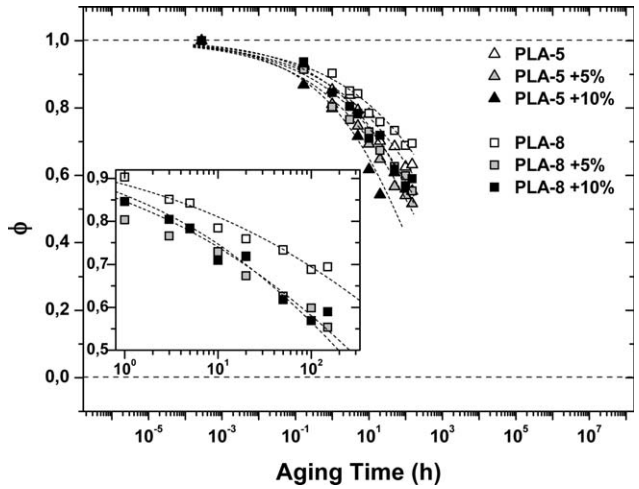

FIG. 8. Recovery function from enthalpy recovery versus ageing time for studied materials. Dashed lines correspond to the fits.

authors that the cooperativity volume is related to the number and the nature of inter-chains bonds. This includes in particular the studies evidencing an increase of cooperativity length with the increase of hydrogen bonds in the system [71, 72]. Nakanishi et al. [73] even proposed to express the cooperativity, the fragility index, and the glass transition temperature as a function of the number of hydroxyl groups for homologous structure series of molecules. Furthermore, it is speculated that, in nanoconfined environments, the exfoliated nanoclays can anchor polymer chains leading to an increase of cooperativity [74]. The decrease of weak bond interactions between polymer chains can probably lead to a decrease the CRR size. This is assumed by Lixon et al. [75] who suggest that the relaxation is less cooperative when covalent bonds become predominant over Van der Waals bonds and by Grigoras et al. [76] who used pending electron donor and electron acceptor groups on the same polymeric chain to create intramonomeric electron transfer and limit cooperativity. Arabeche et al. [77, 78] also showed in confined nanolayers that the annihilation of π-stacking in polycarbonate results in a significant decrease of cooperativity. All these observations together would show that the occurrence of noncovalent intermacromolecular interactions favors cooperative chain motions. We conclude for the case of plasticized PLA, that interactions between PLA chains are hindered by the breaking of macromolecular interaction due to the intercalation of plasticizer molecules and by the free volume increase caused by the plasticizer addition. However, according to our results, no difference can be noticed between PLA-5/TA and PLA-8/ATBC systems. In this case, the effect seems to be independent from the chemical nature of the plasticizer and the stereochemistry of PLA.

CONCLUSION

A rigorous experimental procedure is established for investigating ageing of amorphous PLA samples plasticized with TA and ATBC without loss of plasticizer due to evaporation or thermal degradation. The distance of the ageing temperature from the glass transition temperature of the plasticized materials is thoroughly controlled at equal for all samples of the sample set. This allows for comparison among different types of plasticizers

and has to be distinguished from the classical ageing at ambient temperature not taking into account the change of molecular dynamics related to the glass transition decrease caused by plasticizing. Using the Donth's approach, the CRR lengths have been calculated. The CRR volume at T_α decreased of 60% for both PLA-5 10% TA and PLA-8 10% ATBC. This evidences higher macromolecular mobility at the glass transition due to breakage of polymer/polymer intermolecular interactions. The determination of the recovery function from the physical ageing study shows the role of the plasticizer during physical ageing. Even in the glassy state, the molecular mobility is accelerated by the plasticizer. The comparison of both plasticizers shows better thermal stability of ATBC compared to TA but no difference in the reduction of the CRR size and changes in the enthalpy recovery function. The chemical nature of the plasticizers chosen in this work did not impact on the changes in molecular mobility. The comparison of both PLA grades containing a different quantity of mesolactide did not show any variation, either. It can be concluded that the occurrence of small differences in stereochemistry and average molecular mass does not impact physical ageing and molecular mobility of PLA.

ACKNOWLEDGMENTS

The authors will like to thank A. Maros, S. Dramé, Dr. C. Courgneau, and Dr. F. Hamonic for their experimental contributions.

REFERENCES

1. N. Najafi, M.C. Heuzey, and P.J. Carreau, *Polym. Eng. Sci.*, **53**, 1053 (2013).
2. S. Domenek, C. Courgneau, and V. Ducruet, "Characteristics and applications of PLA," In: *Biopolymers: Biomedical and Environmental Applications*, S. Kalia and L. Avérous, Eds., Wiley, Hoboken, NJ, 183 (2011).
3. A. Ruellan, S. Domenek, and V. Ducruet, "Plasticization of poly (lactide)," In: *Poly(lactic acid) science and technology*, A. Jiménez, R.A. Ruseckaite, M.A. Peltzer, Eds., Royal Chemical Society, London, UK (2014).
4. H. Liu and J. Zhang, *J. Polym. Sci. Part B: Polym. Phys.*, **49**, 1051 (2011).
5. N. Burgos, V.P. Martino, and A. Jiménez, *Polym. Degrad. Stab.*, **98**, 651 (2013).
6. S.-L. Yang, Z.-H. Wu, B. Meng, and W. Yang, *J. Polym. Sci. Part B: Polym. Phys.*, **47**, 1136 (2009).
7. N. Ljungberg, T. Andersson, and B. Wesslén, *J. Appl. Polym. Sci.*, **88**, 3239 (2003).
8. C. Courgneau, O. Vitrac, V. Ducruet, and A.-M. Riquet, *J. Magn. Reson.*, **233**, 37 (2013).
9. F. Hassouna, J.-M. Raquez, F. Addiego, V. Toniazzo, P. Dubois, and D. Ruch, *Eur. Polym. J.*, **48**, 404 (2012).
10. A.J. Kovacs, *Fortschr. Der Hochpolymeren-Forschung*, **3**, 394 (1964).
11. A.J. Kovacs, *Rheol. Acta*, **5**, 262 (1966).
12. L.C.E. Struik, Physical Ageing in Amorphous Polymers and Other Materials, Elsevier Scientific Pub. Co., Distributors for the U.S. and Canada, Elsevier North-Holland, Amsterdam, New York (1978).
13. A.Q. Tool, *J. Am. Ceram. Soc.*, **29**, 240 (1946).
14. O.S. Narayanaswamy, *J. Am. Ceram. Soc.*, **54**, 491 (1971).
15. C.T. Moynihan, *Ann. NY. Acad. Sci.*, **279**, 15 (1976).
16. A.J. Kovacs, J.J. Aklonis, J.M. Hutchinson, and A.R. Ramos, *J. Polym. Sci.: Polym. Phys. Ed.*, **17**, 1097 (1979).
17. G.B. Mckenna, *J. Non-Cryst. Solids.*, 172, **756** (1994).
18. G.B. Mckenna, Y. Leterrier, and C.R. Schultheisz, *Polym. Eng. Sci.*, **35**, 403 (1995).
19. S.L. Simon, D.J. Plazek, J.W. Sobieski, and E.T. McGregor, *J. Polym. Sci. Part B: Polym. Phys.*, **35**, 929 (1997).
20. G.B. Mckenna, M.G. Vangel, A.L. Rukhin, S.D. Leigh, B. Lotz, and C. Straupe, *Polymer*, **40**, 5183 (1999).
21. J. Mijović, L. Nicolais, A. D'amore, and J.M. Kenny, *Polym. Eng. Sci.*, **34**, 381 (1994).
22. J.M. Hutchinson, *Prog. Polym. Sci.*, **20**, 703 (1995).
23. P.A. O'Connell and G.B. Mckenna, *J. Chem. Phys.*, **110**, 11054 (1999).
24. V.M. Boucher, D. Cangialosi, A. Alegría, and J. Colmenero, *Macromolecules*, **44**, 8333 (2011).
25. D. Cangialosi, V.M. Boucher, A. Alegría, and J. Colmenero, *Soft Matter*, **9**, 8619 (2013).
26. A.D. Drozdov, *J. Polym. Sci. Part B: Polym. Phys.*, **39**, 1312 (2001).
27. G. Adam and J.H. Gibbs, *J. Chem. Phys.*, **43**, 139 (1965).
28. H. Cai, V. Dave, R.A. Gross, and S.P. McCarthy, *J. Polym. Sci. Part B: Polym. Phys.*, **34**, 2701 (1996).
29. P. Pan, B. Zhu, T. Dong, K. Yazawa, T. Shimizu, M. Tansho, and Y. Inoue, *J. Chem. Phys.*, **129**, 184902 (2008).
30. T. Zhang, J. Hu, Y. Duan, F. Pi, and J. Zhang, *J. Phys. Chem. B*, **115**, 13835 (2011).
31. M. Kwon, S.C. Lee, and Y.G. Jeong, *Macromol. Res.*, **18**, 346 (2010).
32. P. Pan, B. Zhu, and Y. Inoue, *Macromolecules*, **40**, 9664 (2007).
33. N. Delpouve, A. Saiter, J.F. Mano, and E. Dargent, *Polymer*, **49**, 3130 (2008).
34. N. Delpouve, A. Saiter, and E. Dargent, *Eur. Polym. J.*, **47**, 2414 (2011).
35. N. Delpouve, M. Arnoult, A. Saiter, E. Dargent, and J.-M. Saiter, *Polym. Eng. Sci.*, **54**, 1144 (2014).
36. A.A. Lacey, D.M. Price, and M. Reading, *Modulated Temperature Differential Scanning Calorimetry*, M. Reading, D.J. Hourston, Eds., Springer, Netherlands **1** (2006).
37. S. Weyer, A. Hensel, and C. Schick, *Thermochim. Acta*, 304, **267** (1997).
38. M. Lé-Magda, E. Dargent, J.A.S. Puente, A. Guillet, E. Font, and J.-M. Saiter, *J. Appl. Polym. Sci.*, **130**, 786 (2013).
39. R. Crétois, L. Delbreilh, E. Dargent, N. Follain, L. Lebrun, and J.M. Saiter, *Eur. Polym. J.*, **49**, 3434 (2013).
40. J.M. Saiter, J. Grenet, E. Dargent, A. Saiter, and L. Delbreilh, *Macromol. Symp.*, **258**, 152 (2007).
41. R. Acioli-Moura and X.S. Sun, *Polym. Eng. Sci.*, **48**, 829 (2008).
42. S. Saeidlou, M.A. Huneault, H. Li, and C.B. Park, *Prog. Polym. Sci.*, **37**, 1657 (2012).
43. M. Baiardo, G. Frisoni, M. Scandola, M. Rimelen, D. Lips, K. Ruffieux, and E. Wintermantel, *J. Appl. Polym. Sci.*, **90**, 1731 (2003).

44. M. Murariu, A. Da Silva Ferreira, M. Alexandre, and P. Dubois, *Polym. Adv. Technol.*, **19**, 636 (2008).
45. C. Courgneau, S. Domenek, A. Guinault, L. Avérous, and V. Ducruet, *J. Polym. Environ.*, **19**, 362 (2011).
46. V. Arias, A. Höglund, K. Odelius, and A.-C. Albertsson, *J. Appl. Polym. Sci.*, **130**, 2962 (2013).
47. C. Courgneau, S. Domenek, R. Lebossé, A. Guinault, L. Avérous, and V. Ducruet, *Polym. Int.*, **61**, 180 (2012).
48. M. Scatto, E. Salmini, S. Castiello, M.-B. Coltelli, L. Conzatti, P. Stagnaro, L. Andreotti, and S. Bronco, *J. Appl. Polym. Sci.*, **127**, 4947 (2013).
49. N. Ljungberg and B. Wesslén, *J. Appl. Polym. Sci.*, **86**, 1227 (2002).
50. R. Salazar, S. Domenek, C. Courgneau, and V. Ducruet, *Polym. Degrad. Stab.*, **97**, 1871 (2012).
51. N. Ljungberg and B. Wesslén, *Polymer* **44**, 7679 (2003).
52. E. Donth, *J. Polym. Sci. Part B: Polym. Phys.*, **34**, 2881 (1996).
53. E. Donth, *J. Non-Crystal. Solids*, **53**, 325 (1982).
54. J. Korus, E. Hempel, M. Beiner, S. Kahle, and E. Donth, *Acta Polym.*, **48**, 369 (1997).
55. E. Hempel, G. Hempel, A. Hensel, C. Schick, and E. Donth, *J. Phys. Chem. B* **104**, 2460 (2000).
56. T.A. Tran, S. Saïd, and Y. Grohens, *Compos. A*, **36**, 461 (2005).
57. D. Cangialosi, A. Alegría, and J. Colmenero, *Phys. Rev. E*, **76**, 011514 (2007).
58. N. Delpouve, C. Lixon, A. Saiter, E. Dargent, and J. Grenet, *J. Thermal Anal. Calorimetry*, **97**, 541 (2009).
59. A. Saiter, D. Prevosto, E. Passaglia, H. Couderc, L. Delbreilh, and J.M. Saiter, *Phys. Rev. E*, **88**, 042605 (2013).
60. Y. Furushima, K. Ishikiriyama, and T. Higashioji, *Polymer*, **54**, 4078 (2013).
61. T. Sasaki, T. Uchida, and K. Sakurai, *J. Polym. Sci. Part B: Polym. Phys.*, **44**, 1958 (2006).
62. G. Dlubek, V. Bondarenko, J. Pionteck, M. Supej, A. Wutzler, and R. Krause-Rehberg, *Polymer*, **44**, 1921 (2003).
63. C. Lixon Buquet, F. Hamonic, A. Saiter, E. Dargent, D. Langevin, and Q.T. Nguyen, *Thermochim. Acta*, **509**, 18 (2010).
64. I.M. Hodge, *Science*, **267**, 1945 (1995).
65. Y.P. Koh and S.L. Simon, *Macromolecules*, **46**, 5815 (2013).
66. J.L.G. Ribelles, R. Diaz-Calleja, R. Ferguson, and J.M.G. Cowie, *Polymer*, **28**, 2262 (1987).
67. Y.P. Koh and S.L. Simon, *J. Polym. Sci. Part B: Polym. Phys.*, **46**, 2741 (2008).
68. J.D. Stevenson, J. Schmalian, and P.G. Wolynes, *Nat. Phys.*, **2**, 268 (2006).
69. S. Capaccioli, G. Ruocco, and F. Zamponi, *J. Phys. Chem. B*, **112**, 10652 (2008).
70. R. Casalini, D. Fragiadakis, and C.M. Roland, *Macromolecules*, **44**, 6928 (2011).
71. M. Paluch, S. Pawlus, A. Grzybowski, K. Grzybowska, P. Włodarczyk, and J. Zioło, *Phys. Rev. E*, **84**, 052501 (2011).
72. N. Delpouve, A. Vuillequez, A. Saiter, B. Youssef, and J.M. Saiter, *Phys. B: Condens. Matter*, **407**, 3561 (2012).
73. M. Nakanishi and R. Nozaki, *Phys. Rev. E*, **84**, 011503 (2011).
74. A. Leszczynska and K. Pielichowski, *J. Thermal Anal. Calorim.*, **93**, 677 (2008).
75. C. Lixon, N. Delpouve, A. Saiter, E. Dargent, and Y. Grohens, *Eur. Polym. J.*, **44**, 3377 (2008).
76. C.V. Grigoras and A.G. Grigoras, *J. Thermal Anal. Calorim.*, **103**, 661 (2010).
77. K. Arabeche, L. Delbreilh, R. Adhikari, G.H. Michler, A. Hiltner, E. Baer, and J.-M. Saiter, *Polymer*, **53**, 1355 (2012).
78. K. Arabeche, L. Delbreilh, J.-M. Saiter, G. H. Michler, R. Adhikari, and E. Baer, *Polymer*, **55**, 1546 (2014).